Available online at www.sciencedirect.com
ScienceDirect
Tectonophysics 424 (2006) 271–289
TECTONOPHYSICS
www.elsevier.com/locate/tecto

Elastic and inelastic triggering of earthquakes in the North Anatolian Fault zone

Francisco Lorenzo-Martín [a,*], Frank Roth [b], Rongjiang Wang [b]

[a] *Institute of Geology, Mineralogy and Geophysics, Ruhr University Bochum, D-44780 Bochum, Germany*
[b] *GeoForschungsZentrum Potsdam (GFZ), Telegrafenberg, D-14467 Potsdam, Germany*

Received 18 July 2005; received in revised form 26 November 2005; accepted 25 March 2006
Available online 9 August 2006

Abstract

Deformation models used to explain the triggering mechanism often assume pure elastic behaviour for the crust and upper mantle. In reality however, the mantle and possibly the lower crust behave viscoelastically, particularly over longer time scales. Consequently, the stress field of an earthquake is in general time-dependent. In addition, if the elastic stress increase were enough to trigger a later earthquake, this triggered event should occur instantaneously and not many years after the triggering event. Hence, it is appropriate to include inelastic behaviour when analysing stress transfer and earthquake interaction.

In this work, we analyse a sequence of 10 magnitude $M_s > 6.5$ events along the North Anatolian Fault between 1939 and 1999 to study the evolution of the regional Coulomb stress field. We investigate the triggering of these events by stress transfer, taking viscoelastic relaxation into account. We evaluate the contribution of elastic stress changes, of post-seismic viscoelastic relaxation in the lower crust and mantle, and of steady tectonic loading to the total Coulomb stress field. We analyse the evolution of stress in the region under study, as well as on the rupture surfaces of the considered events and their epicentres. We study the state of the Coulomb stress field before the 1999 İzmit and Düzce earthquakes, as well as in the Marmara Sea region.

In general, the Coulomb stress failure criterion offers a plausible explanation for the location of these events. However, we show that using a purely elastic model disregards an important part of the actual stress increase/decrease. In several cases, post-seismic relaxation effects are important and greater in magnitude than the stress changes due to steady tectonic loading. Consequently, viscoelastic relaxation should be considered in any study dealing with Coulomb stress changes.

According to our study, and assuming that an important part of the rupture surface must be stressed for an earthquake to occur, the most likely value for the viscosity of the lower crust or mantle in this region is $5 \cdot 10^{17}$–10^{18} Pa·s. Our results cannot rule out the possibility of other time-dependent processes involved in the triggering of the 1999 Düzce event. However, the stress increase due to viscoelastic relaxation brought 22% of the 1999 Düzce rupture area over the threshold value of $\Delta\sigma_c \geq 0.01$ MPa (0.1 bar), and took the whole surface closer to failure by an average of 0.2 MPa. Finally, we argue that the Marmara Sea region is currently being loaded with positive Coulomb stresses at a much faster rate than would arise exclusively from steady tectonic loading on the North Anatolian Fault.

Keywords: Coulomb stress; Triggering; North Anatolian Fault; Dislocation theory; Rheology; Viscosity

* Corresponding author. Current address: GeoForschungsZentrum Potsdam (GFZ), Telegrafenberg, D-14467 Potsdam, Germany. Tel.: +49 331 288 1285; fax: +49 331 288 1204.
E-mail address: lorenzo@gfz-potsdam.de (F. Lorenzo-Martín).

0040-1951/$ - see front matter © 2006 Elsevier B.V. All rights reserved.
doi:10.1016/j.tecto.2006.03.046

1. Introduction

The North Anatolian Fault zone (NAF) is an almost pure dextral 1500 km long fault zone running along the north of Turkey (Fig. 1). During the last century, several strong earthquakes have taken place along the NAF. These events or subsets of them have been the subject of numerous studies (Mogi, 1968; Toksöz et al., 1979; Purcaru and Berckhemer, 1982; Roth, 1988; Stein et al., 1997). There are several reasons for the interest: first, the events provide an unequalled possibility to analyse how the occurrence of an earthquake may trigger additional shocks. Second, the number of field investigations provides a valuable and still increasing amount of information. Third, recent events appear to be propagating westwards, with the M_w=7.4 İzmit and the M_w=7.1 Düzce earthquakes in 1999 as the most recent and westernmost events. If this sense of propagation continues, a strong shock west of the İzmit–Düzce rupture can be expected (Hubert-Ferrari et al., 2000; Parsons et al., 2000; Parsons, 2004). This region would be the Marmara Sea, just south of Istanbul, a mega-city with 12 million inhabitants. A strong earthquake in this region would therefore have catastrophic consequences, both in loss of life and monetary costs.

The triggering of earthquakes by stress transfer has been analysed by numerous authors (Healy et al., 1968; Raleigh et al., 1972; Harris, 1998; Belardinelli et al., 1999; King and Cocco, 2001; Belardinelli et al., 2003; Hardebeck, 2004; Freed, 2005; Steacy et al., 2005). Previous deformation models often assume purely elastic behaviour for the crust and upper mantle, and therefore the crust instantaneously responds to the motion on the rupture. When using the elastic approach, any time dependence of the deformation might be attributed to time-dependent fault slip (Kasahara, 1975; Linde and Silver, 1989; Barrientos et al., 1992). Several studies have shown good correlation between calculated positive elastic (coseismic) stress change and the location of aftershocks (Reasenberg and Simpson, 1992; Stein et al., 1992; King et al., 1994; Nalbant et al., 1996; Toda et al., 1998; Deng et al., 1999; Ma et al., 2005; Nostro et al., 2005), as well as the triggering of moderate to large earthquakes (King et al., 1994; Stein et al., 1994; Harris et al., 1995; Stein et al., 1997; Nalbant et al., 1998; Stein, 1999; Nalbant et al., 2002; McCloskey et al., 2005; Nalbant et al., 2005b).

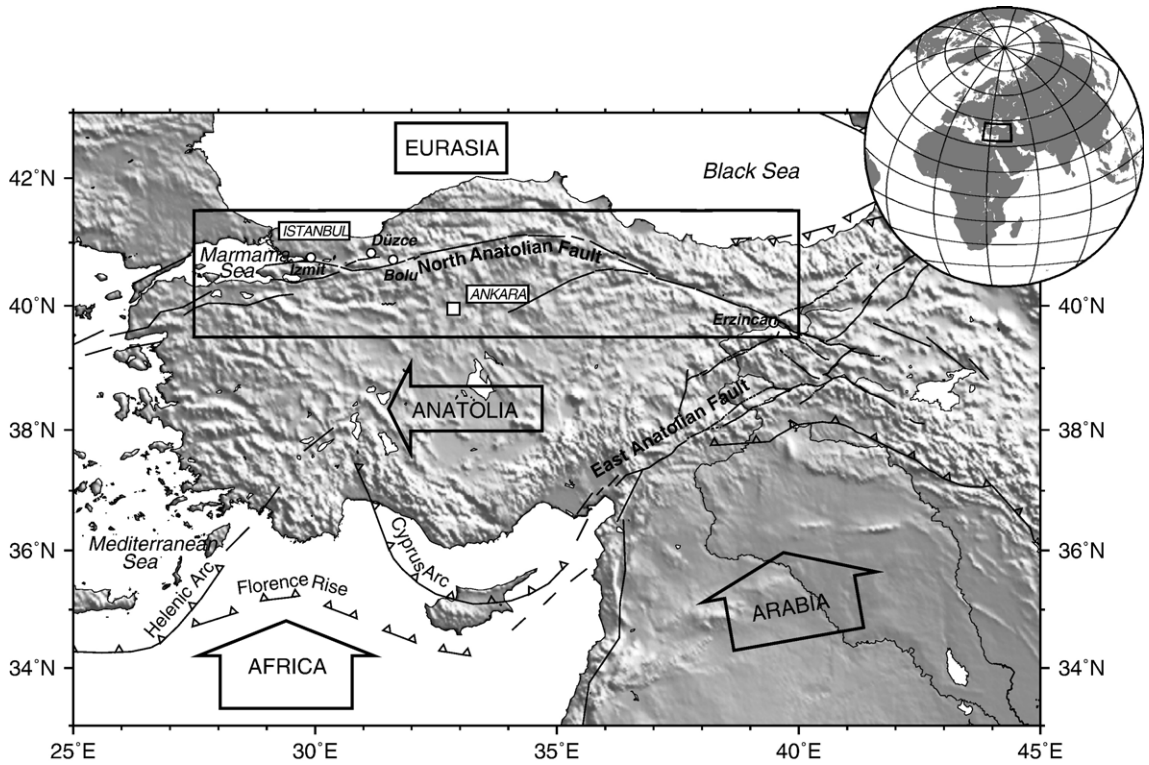

Fig. 1. Map showing the major tectonic elements of Turkey. Anatolia is forced to move towards the Aegean subduction zone, moving along the North and East Anatolian faults. The box shows our study area.

However, in the real Earth, the mantle and possibly the lower crust behave as an inelastic body, that is, any imposed stress will relax with time. The crust will first deform as an elastic body, but later deformation will continue because of stress relaxation (Thatcher and Rundle, 1984). Since inelastic stress relaxation also leads to redistribution of the stress, it is necessary to include inelastic behaviour when analysing stress transfer and earthquake interaction. Also, an important limitation of the elastic/coseismic stress change approach is that it cannot explain time delays of the triggered events. Post-seismic stress changes due to viscous relaxation in the lower crust and/or upper mantle have also been successfully used to explain aftershock distribution and the triggering of later events (Deng et al., 1999; Freed and Lin, 2001; Zeng, 2001; Pollitz and Sacks, 2002). However, only pairs of events have been considered so far to analyse whether, and how, the Coulomb stress is increased by post-seismic relaxation.

In the present study, we investigated a sequence of 10 magnitude $M_s > 6.5$ earthquakes (Table 1 and Fig. 2) that have occurred on the NAF since 1939. In contrast to Roth (1988), the geographical region considered here brackets the area from the Marmara Sea in the west to east of Erzincan. We also took into account the details in orientation and geometry of the different ruptures. In addition, further studies carried out in the last few years have allowed us to consider more realistic values than those from Roth (1988) for the medium properties and stratification, as well as for the stress build-up due to plate motion on the NAF.

The last strong events before 1939 in this region took place in the 18th century (Ambraseys and Finkel, 1995; Sengör et al., 2005). We can assume therefore that the 1939 event was the first in a new seismic cycle, and that the stress field in the region has been homogenized by steady tectonic loading. Moderate events may have a locally important influence on the stress field. However, information about their location and effects is usually not accurate enough, especially for older events and/or on the centre and eastern part of the NAF. Assuming 1939 as a start for the calculations and $M_s > 6.5$ as the magnitude threshold is a good compromise to consider a significantly long seismic series and information reliable enough for the correct modelling of the considered earthquakes. We studied the changes in the Coulomb stress field from the beginning of the sequence to the present day. Previous similar works (Stein et al., 1997; Cakir et al., 2003; Muller et al., 2003) considered the instantaneous response to the events and the effects of stress change due to tectonic loading from steady slip beneath the NAF. In the present study, we additionally take into account the effect of viscoelastic relaxation in the lower crust and upper mantle. We evaluated the importance of the three processes on the total stress field.

We also analysed the time evolution of the Coulomb stress at the epicentres of the shocks, as well as the state on the rupture surfaces immediately before the earthquakes, under different assumptions. We considered the current situation in the Marmara Sea and extrapolated it to the year 2010 to evaluate the rate at which viscoelastic relaxation is increasing the stresses in the region,

Table 1
Parameters of the sequence of earthquakes used

Date	GMT	Lat. (°N)	Lon. (°E)	M_s	M_o (Nm)	References
1939 26 Dec	23:57	39.80	39.38	8.0	$4.11 \cdot 10^{20}$	(3), (4), (6), (8)
1942 20 Dec	14:03	40.66	36.35	7.3	$1.74 \cdot 10^{19}$	(3), (4), (6), (8)
1943 26 Nov	22:20	41.05	33.72	7.6	$2.51 \cdot 10^{20}$	(3), (4), (6), (8)
1944 01 Feb	03:23	41.00	33.22	7.6	$1.48 \cdot 10^{20}$	(3), (4), (6), (8)
1951 13 Aug	18:33	40.86	32.68	6.7	$2.12 \cdot 10^{19}$	(1), (4), (5)
1957 26 May	06:33	40.58	31.00	7.2	$1.35 \cdot 10^{19}$	(3), (4), (6), (8)
1967 22 Jul	16:56	40.57	30.80	7.3	$2.82 \cdot 10^{19}$	(2), (3), (4), (6), (8), (14)
1992 13 Mar	17:19	39.71	39.60	6.9	$1.14 \cdot 10^{19}$	(6), (7), (9), (10)
1999 17 Aug	00:01	40.70	29.91	7.8	$2.15 \cdot 10^{20}$	(12), (13), (14)
1999 12 Nov	16:57	40.818	30.198	7.3	$4.67 \cdot 10^{19}$	(11), (12), (16), (17)

Epicentral coordinates are from Dewey (1976) until 1967, with the exception of the 1943 event, for which Dewey's epicentral coordinates appear to be too far East (Ambraseys, 1970; Alsan et al., 1976; Saroglu et al., 1992). For this event and the more recent ones, we used the coordinates provided by the Earthquake Research Directorate (ERD), Seismological Division, Turkey. M_s values are from the USGS. M_o values correspond to the geometry and slip distribution used in the present work, comparable to those of Stein et al. (1997). The references used are: (1) Pinar, 1953; (2) Ambraseys and Zatopek, 1969; (3) Ambraseys, 1970; (4) Dewey, 1976; (5) Barka and Kadinsky-Cade, 1988; (6) Saroglu et al., 1992; (7) Pinar et al., 1994; (8) Barka, 1996; (9) Nalbant et al., 1996; (10) Grosser et al., 1998; (11) Ayhan et al., 2001; (12) Tibi et al., 2001; (13) Wright et al., 2001; (14) Barka et al., 2002; (15) Muller et al., 2003; (16) Utkucu et al., 2003; and (17) Umutlu et al., 2004.

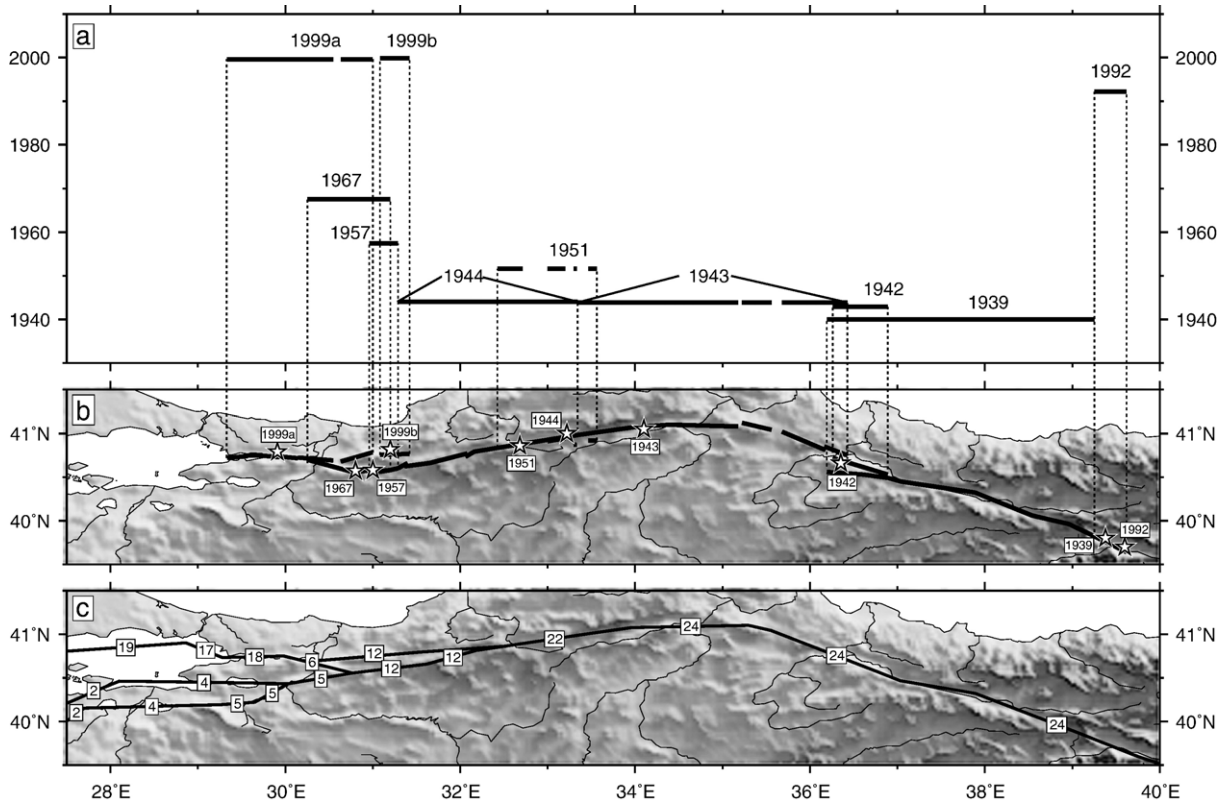

Fig. 2. Space–time migration of the 10 considered M_s>6.5 earthquakes along the NAF during the period 1939 to 1999. Thick lines in (a) and (b) display the events. Stars indicate the epicentres of the shocks in the sequence (Dewey, 1976, ERD Turkey, USGS). Lines in (c) represents the geometry of the North Anatolian Fault used in the calculations. The values are the amount of slip/year on the segments in mm/a (Armijo et al., 2003; Flerit et al., 2003, 2004).

information that may be useful for seismic-hazard assessment in this region.

2. Tectonic setting

The tectonic setting of the study region is dominated by the collision of the Arabian and African plates against the Eurasian and Anatolian ones (Fig. 1). The Arabian and African plates move approximately northward against the relatively stable Eurasian plate, causing the Anatolian block to move westwards from the East Anatolian Convergence Zone onto the oceanic lithosphere of the Eastern Mediterranean Sea (Sengör et al., 1985; Sengör et al., 2005). This movement changes its direction to southwest in West Anatolia and the Aegean Sea, so that the large scale result is a counter-clockwise rotation of the Anatolian Plate (McKenzie, 1972; Jackson and McKenzie, 1988; McClusky et al., 2000). This relative westward movement of the Anatolian Plate generates strike slip on both the NAF and the East Anatolian Fault zone (EAF). Along most of the NAF, the right-lateral slip has a rate of 24±1 mm/a (McClusky et al., 2000; Flerit et al., 2004).

The NAF splits into three different branches at its westernmost part. About 80% of the total slip accommodates on the northern branch and the remaining 20% is distributed between the other two (Flerit et al., 2003). The northern branch crosses the Marmara Sea, linking the İzmit segment in the east with the Ganos fault in the west (Le Pichon et al., 2001; Gokasan et al., 2003; Armijo et al., 2005). The NAF in the Marmara Sea consists of two main parts: a western one, about 120 km long and striking N265°E, and a 50 km long eastern segment, striking N280°E. These two segments were the probable location of several strong and damaging historical earthquakes, the latter of which took place in 1754, 1766 and 1894 (Ambraseys and Finkel, 1991; Ambraseys, 2002; Parsons, 2004). The Marmara Sea region has also been identified as a seismic gap (Hubert-Ferrari et al., 2000).

3. Methodology

During the last decade, Coulomb stress modelling has become a popular and accepted tool to analyse the conditions under which earthquakes occur (King et al., 1994; Stein et al., 1997; Zeng, 2001; Muller et al., 2003; Lin and Stein, 2004). In this study, we computed stress field produced by dislocation sources embedded in a mixed elastic/inelastic layered half-space (Wang et al., 2003, 2006). We use the elastic–viscoelastic correspondence principle (Christensen, 1982), which states that a linear viscoelastic boundary-value problem can be solved by adopting the associated elastic solutions where the elastic moduli are replaced by the Laplace or Fourier transformed complex moduli. The time-domain solutions are then obtained using the inverse Fast Fourier Transform. A comparison between the method used here and the one published by Fernández et al. (1996) can be found in Wang (2005). Most significantly, Wang's approach corrects an inconsistency in the former formulation when including gravity effects to calculate the deformation (Fernández and Rundle, 2004; Wang, 2005; Wang et al., 2006). Another tool has been developed by Pollitz (1992, 1997), for the calculation of gravitational viscoelastic post-seismic relaxation on a layered spherical Earth. Some differences between results by both his and Wang's approach can be found at the late post-seismic period (Wang, 2005), but they are not relevant for the present study.

Once the components of the stress tensor have been calculated, the Coulomb stress change ($\Delta\sigma_c$) is given by:

$$\Delta\sigma_c = \Delta\tau + \mu'\Delta\sigma_N, \tag{1}$$

where τ is the shear stress, σ_N is the normal stress and μ' is the effective (or apparent) coefficient of friction. When Coulomb stresses surpass a certain critical value, failure occurs. Normal and shear stresses are positive when the fault is unclamped and in the corresponding slip direction respectively, so that both positive normal and shear stresses encourage failure. The orientation of a known fault can be used to define the reference system to calculate normal and shear stresses. When no target fault is considered, Coulomb stresses can be calculated on so called "optimally oriented fault planes", obtaining the direction in which Coulomb stress is at its maximum. This approach is useful to analyse the correlation between Coulomb stress changes and aftershock distribution, since it can be assumed that a sufficient number of small faults with all orientations exist, and that the faults optimally oriented for failure will be most likely to slip in small earthquakes. The calculation of the optimum directions, however, implies knowledge of the pre-existing regional stress field (King et al., 1994).

The effective coefficient of friction is often assumed to be constant in a given area, and it is utilized to include the unknown effects of pore-fluid pressure in the crust (Harris, 1998). This parameter is not a material constant, as often implicitly assumed, and its relationship with pore pressure is not simple (Beeler et al., 2000; Cocco and Rice, 2002). A common simplification is to assume that the change in pore pressure is proportional to the normal stress. Under this assumption, μ' is related to the friction coefficient μ through the Skempton coefficient B as follows:

$$\mu' = \mu(1-B), \tag{2}$$

where B describes the presence of fluids in rock, with $B=0$ for completely drained rocks and $B=1$ for the maximum possible presence of fluids. A coefficient of friction of $\mu=0.85$ from laboratory values (Byerlee, 1978) and a moderate pore pressure ($B\sim0.5$) lead to a value of $\mu'=0.4$. However, if fluids are expelled from the fault zone, the value for μ' will increase up to that of μ.

4. Model parameters

The layered model used for our calculations is described by the rock parameters summarised in Fig. 3 (Milkereit et al., 2000; Milkereit et al., 2004). We considered a Poisson's ration of 0.25. Concerning the rheological properties, we first considered a medium with a strong viscoelastic lower crust and a weak viscoelastic mantle (hereinafter Model 1). However, although other authors have favoured similar stratification for their studies (e.g. Freed and Lin, 2001; Pollitz and Sacks, 2002), there is also the possibility that the most appropriate description of the medium is the opposite, with a weak lower crust and a strong mantle (Deng et al., 1998; Deng et al., 1999; Zeng, 2001), or that the lithosphere should be considered elastic over its whole depth (Casarotti and Piersanti, 2003). For this reason, we also considered two models incorporating these options (respectively Model 2 and Model 3). In all the cases, viscoelastic layers are modelled as Maxwell bodies. According to recent studies, other rheological models could be more adequate to analyse post-seismic relaxation processes, like the Standard Linear Solid rheology (Cohen, 1982; Pollitz et al., 1998) or power-

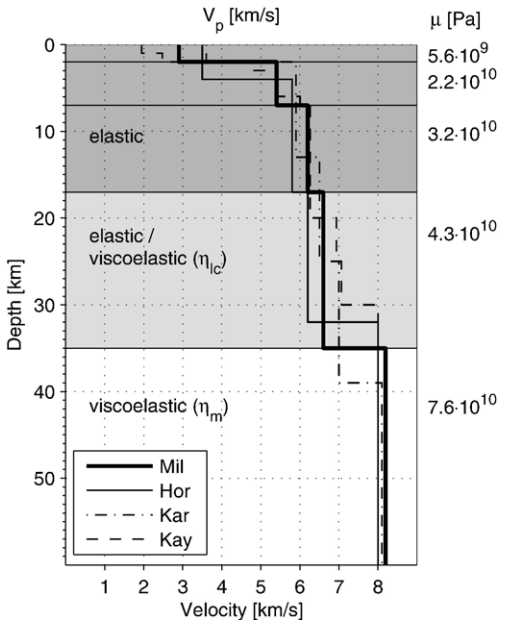

Fig. 3. Parameters of the horizontally stratified medium. The same stratification values have been applied for different tectonically active areas along the NAF (Milkereit et al., 2000, 2004, thick line). Results from other studies are also shown for comparison (Karahan et al., 2001; Horasan et al., 2002; Kaypak and Eyidogan, 2005). The lower crust and the mantle have variable viscosities η_{lc} and η_m, respectively.

law, non-linear rheologies (Pollitz et al., 2001; Freed and Bürgmann, 2004). However, from the present data we are not able to discern among different rheologies. For this reason, we prefer to use the simplest and most used linear Maxwell rheology, instead of more complicated models that would add additional unknowns to our analysis.

Fault rupture locations and geometry, as well as slip distribution, were obtained from tectonic and geological maps and published field observations (see Table 1). We modelled the tectonic stress loading with steady slip over the depth range 17 to 100 km, using the deep dislocation technique proposed by Savage (1983). The slip increases from zero at 17 km depth to its full magnitude at a depth of 35 km. The magnitude of the slip on the NAF was taken from GPS interpretations (Flerit et al., 2003; Flerit et al., 2004). Fig. 2c displays the exact amount of annual fault slip used to model the different segments of the NAF.

With these parameters, we carried out calculations for a grid of 81×501 points, with a spacing of approximately 2 km, covering the study region outlined in Fig. 1. We also calculated Coulomb stress changes at a 2 km spacing along the segments. For these computations, we considered the full geometry for each rupture segments. However, only horizontal stress components were used for the calculations. Since the most important deformation along the NAF is horizontal, this is a reasonable simplification.

5. Results

Fig. 4 illustrates the evolution of the cumulative Coulomb stress changes on vertical fault planes striking in E–W direction. We choose a fixed strike direction for these calculations instead of using optimally oriented fault planes to facilitate the comparison between different snapshots. For these calculations we used Model 1, with $\mu' = 0.4$ and lower crust and mantle viscosities of $5 \cdot 10^{19}$ Pa·s and 10^{18} Pa·s, respectively. Since most of the large earthquakes along the NAF have an hypocentral depth of 10–15 km (e.g. Sengör et al., 2005), Coulomb stresses were calculated at 10 km depth, regarding this as a realistic depth for earthquake nucleation. Fig. 4a shows the effect of the steady tectonic stress loading over 10 years, to illustrate the influence of this process on the total field. The state of the stress field at the beginning of the sequence is shown in Fig. 4b, where only the elastic response of the medium to the 1939 event is present. The evolution in time is then shown, with snapshots immediately before and after the 1943 event (Fig. 4c and d) and after the 1992 event (Fig. 4e). Fig. 4f displays the stress changes due exclusively to viscoelastic relaxation between 1939 and 1992, to demonstrate the effect this process has on the total stress field. Values near the NAF typically range from 0.3 to 0.5 MPa, greater in magnitude than those corresponding to steady tectonic loading for the same period. After both 1999 events, the situation is the one displayed in Fig. 4g, and the evolution of the field until the present time is shown in Fig. 4h (total stress field) and Fig. 4i (only the viscoelastic relaxation effect).

Fig. 4. Evolution of the Coulomb stress field since 1939. Calculations were made for fault planes striking in an E–W direction, and the results were evaluated for 10 km depth. Black thick lines represent all segments used to model the tectonic loading at the NAF. White lines display ruptured segments and red lines unruptured segments, immediately before their activation. (a) shows the effect of 10 years of steady tectonic loading. The rest of the panels display the situation at different points in time: (b) immediately after the 1939 event; (c) before the 1942 event; (d) after the 1942 event; (e) after the 1992 event; (f) effect of viscoelastic relaxation from 1939 to 1992; (g) after the 1999b event; (h) current state of the Coulomb stress field; (i) effect of viscoelastic relaxation from 1939 to 2005.

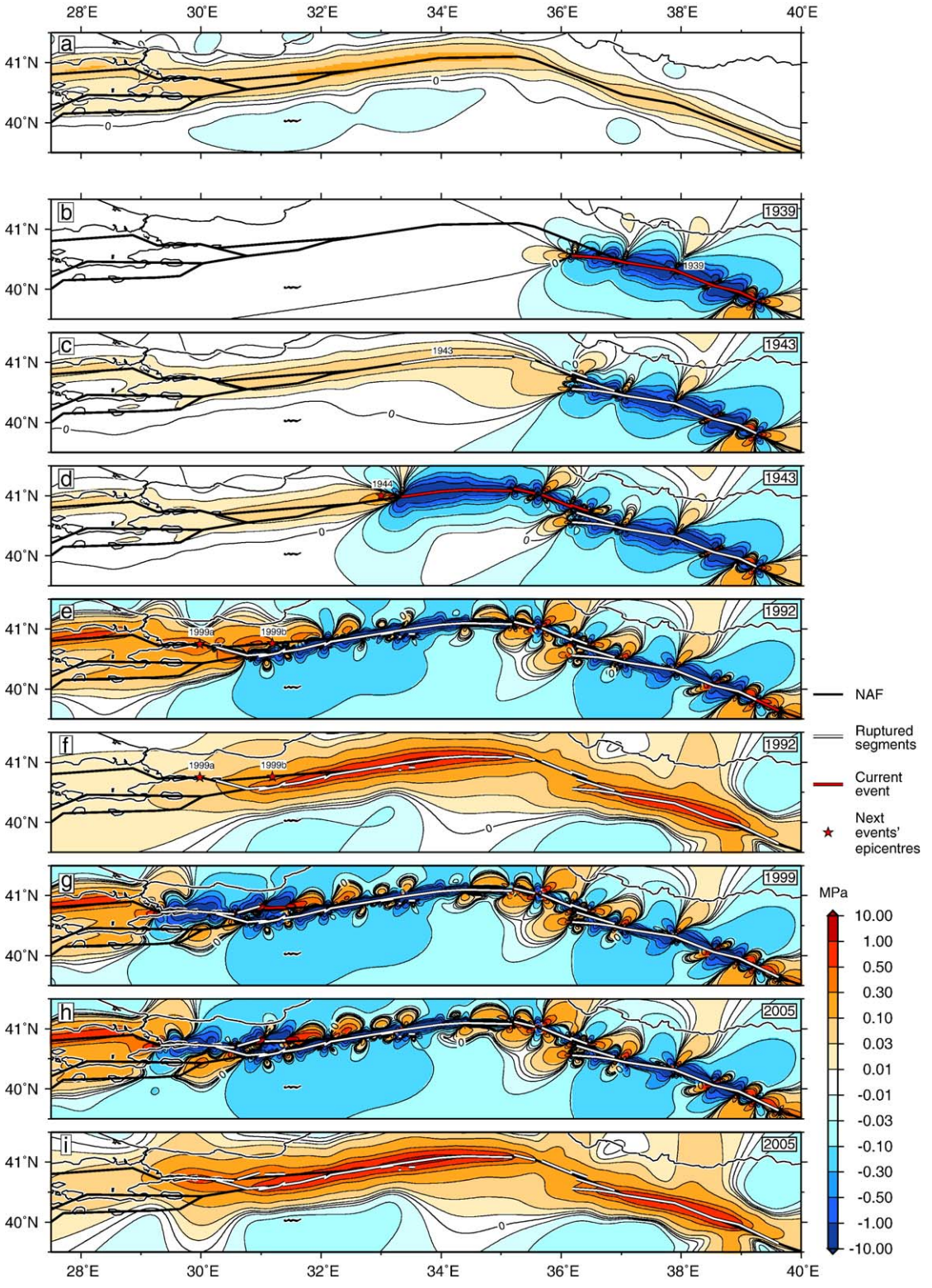
28°E
30°E
32°E
34°E
36°E
38°E
40°E
41°N
40°N
a
b
1939
c
1943
d
1943
e
1992
1999a
1999b
f
1992
1999a
1999b
g
1999
h
2005
i
2005
0
NAF
Ruptured segments
Current event
Next events' epicentres
MPa
10.00
1.00
0.50
0.30
0.10
0.03
0.01
-0.01
-0.03
-0.10
-0.30
-0.50
-1.00
-10.00

Table 2
Maximum and average Coulomb stress changes ($\Delta\sigma_c$) on the ruptures immediately before each event

Viscosity	1942		1943		1944		1951		1957		1967		1992		1999a		1999b	
∞	0.07	−0.67	0.11	0.04	13.37	0.36	−1.52	−3.30	4.52	0.86	0.89	−0.31	3.40	1.29	0.98	0.33	0.57	0.26
$5\cdot10^{17}$ Pa·s	0.17	−0.48	0.23	0.07	13.40	0.37	−1.23	−2.92	4.74	1.00	1.12	−0.16	4.22	1.80	1.14	0.44	0.80	0.50
10^{18} Pa·s	0.15	−0.53	0.20	0.07	13.38	0.37	−1.27	−2.99	4.69	0.97	1.06	−0.20	3.98	1.64	1.10	0.41	0.76	0.46
$5\cdot10^{18}$ Pa·s	0.09	−0.64	0.13	0.05	13.37	0.36	−1.41	−3.18	4.61	0.92	0.98	−0.25	3.68	1.46	1.05	0.39	0.71	0.41
10^{19} Pa·s	0.08	−0.66	0.12	0.05	13.37	0.36	−1.46	−3.24	4.57	0.90	0.94	−0.27	3.63	1.43	1.03	0.37	0.68	0.39
From tect. loading	0.04		0.05		0.05		0.10		0.11		0.22		0.64		0.46		0.56	

Values are for a purely elastic model (infinite viscosity) and for 4 different mantle viscosities, η_m. The ratio with the lower crust viscosity is kept constant at $\eta_{lc}/\eta_m=50$. The last line displays the fraction of the results produced by steady tectonic loading. Results are for Model 1 (see text), and an effective coefficient of friction of 0.4.

5.1. Coulomb stress on the rupture surfaces

We calculated the Coulomb stress change on the rupture surfaces of the events posterior to 1939 and separately assessed the influence of tectonic, elastic and viscoelastic loading. We regarded positive stress values below 0.01 MPa as not significant, since steady tectonic loading can cause such amounts of stress over a very short period of time (Stein et al., 1997). Table 2 compiles values for the maximum and average change stress at the rupture surfaces, while Table 3 displays the percentage of the rupture length with $\sigma_c \geq 0.01$ MPa. The values in both tables display the state immediately before the corresponding event. The values were calculated for Model 1, including results with and without steady tectonic loading, as well as for elastic and viscoelastic media. For the latter, mantle viscosity values from $\eta_m=5\cdot10^{17}$ to 10^{19} Pa·s were considered. We maintained a constant ratio with the lower crust viscosity of $\eta_{lc}/\eta_m=50$ to simplify the analysis. Previous works dealing with southern California propose ratios ranging from 3 to 100 (Deng et al., 1998; Deng et al., 1999; Freed and Lin, 2001; Zeng, 2001; Pollitz and Sacks, 2002), although there is no agreement on whether weak-lower-crust or weak-mantle models are more appropriate.

The joint effect of tectonic, elastic and viscoelastic loading produces positive average Coulomb stress changes on most of the rupture surfaces. The percentage of the rupture surfaces over the threshold value is at its maximum for $\eta_m=5\cdot10^{17}$–10^{18} Pa·s. Three of the ruptures (1942, 1951 and 1967) show negative average Coulomb stress change regardless of the model assumed.

The entire length of the 1951 rupture is in a stress shadow, with the whole surface stressed by less than 0.01 MPa (Table 3). By contrast, the 1957 event shows, independent of the model assumptions, values above this threshold for all its length. The percentage of rupture surface above the threshold for the remaining 7 events depends on the contributions considered for the stress loading, as well as the value of the viscosity when viscoelastic models are used. In general, the influence of viscoelastic relaxation is comparable to that of tectonic loading.

We also carried out calculations using an effective coefficient of friction of 0.6 (Table 4a). This value accounts for a situation where most of the fluids are

Table 3
Percentage of fault rupture showing $\Delta\sigma_c \geq 0.01$ MPa

	Viscosity	1942	1943	1944	1951	1957	1967	1992	1999a	1999b
With tectonic loading	∞	14	93	95	0	100	75	100	85	100
	$5\cdot10^{17}$ Pa·s	29	96	100	0	100	78	100	93	100
	10^{18} Pa·s	21	95	100	0	100	78	100	91	100
	$5\cdot10^{18}$ Pa·s	18	93	95	0	100	75	100	88	100
	10^{19} Pa·s	14	93	95	0	100	75	100	88	100
Without tectonic loading	∞	11	20	52	0	100	70	94	49	7
	$5\cdot10^{17}$ Pa·s	21	59	67	0	100	75	100	81	29
	10^{18} Pa·s	21	44	57	0	100	73	100	81	29
	$5\cdot10^{18}$ Pa·s	14	21	54	0	100	73	94	81	21
	10^{19} Pa·s	11	21	53	0	100	73	94	81	21

Values when including the effects of steady tectonic loading (upper five lines) and when excluding this effects (lower five lines). Model parameters as in Table 2.

Table 4
Percentage of fault rupture with $\Delta\sigma_c \geq 0.01$ MPa

			1942	1943	1944	1951	1957	1967	1992	1999a	1999b
a	With tectonic loading	Elas.	14	94	89	0	100	75	100	88	93
		Visc.	29	98	89	0	100	80	100	93	100
	Without tectonic loading	Elas.	11	21	51	0	100	68	94	57	7
		Visc.	21	35	55	0	100	75	100	81	21
b	With tectonic loading	Visc.	39	94	95	0	100	83	100	94	100
	Without tectonic loading	Visc.	36	33	55	0	100	78	100	78	29
c	With tectonic loading	Visc.	21	95	99	0	100	75	100	88	100
	Without tectonic loading	Visc.	18	33	55	0	100	73	94	81	21

Values for Model 1 with $\mu'=0.6$ (a), for Model 2 with $\mu'=0.4$ (b), and for Model 3 with $\mu'=0.4$ (c). Both elastic and viscoelastic media are considered. The viscosities used are $\eta_m=10^{18}$ Pa·s and $\eta_{lc}/\eta_m=50$ for (a) and (c), and $\eta_{lc}=10^{18}$ Pa·s with $\eta_m/\eta_{lc}=50$ for (b).

expelled from the fault zone. The results differ slightly from those presented above, although changes are not systematic. Most notably, when the total stress field on the 1944 rupture surface is considered, the stressed surface decreases from 100% for $\mu'=0.4$ to 89% for $\mu'=0.6$. The total stress field on the 1942 rupture surface increases, so that the considered percentage increases from 21% for $\mu'=0.4$ to 29% for $\mu'=0.6$. The elastic contribution to the 1999a event is notably larger, increasing the stressed surface from 49% for $\mu'=0.4$ to 57% for $\mu'=0.6$. The viscoelastic contribution to the 1943 event decreases, with the stressed surface decreasing from 44% for $\mu'=0.4$ to 35% for $\mu'=0$.

Results for Model 2 and Model 3 (Table 4b and c) also show localized differences. Most notably, the stressed area on the rupture surfaces of the 1942 and 1967 events increases to 36% and 78%, respectively, for Model 2. In general, the effect of viscoelastic relaxation is smaller for Model 3, as it would expected. The stressed surface of the 1943 rupture decreases to 33% for both Model 2 and Model 3. In the latter model, the stressed surface for the 1943, 1992 and 1999b events decreases in 11%, 6% and 8%, respectively.

5.2. Coulomb stress at the epicentres

Fig. 5 displays the time evolution of the Coulomb stress at the epicentres of the events posterior to 1939. For the 9 epicentres, the effect of the corresponding rupture is a stress release. Also, the epicentres of 8 out of 9 earthquakes are stressed with high $\Delta\sigma_c$ values, although there are differences regarding its magnitude. Epicentres of the events on the central and eastern part of the NAF (1942, 1943 and 1944) were loaded by about 0.1 MPa before the rupture took place. The epicentres for 1957 and 1967, on the other hand, stored stresses up to values around 0.3 MPa, and up to 0.5 MPa for the 1999a and 1999b epicentres, before the earthquakes occurred. The 1992 epicentre was loaded with more than 0.9 MPa immediately before the shock took place.

In general, it can be observed that the increase in magnitude of $\Delta\sigma_c$ due to viscoelastic relaxation is comparable, and in some cases larger, than that due to steady tectonic loading (compare the thin dashed and solid lines, Fig. 5).

The location of epicentres, especially the earlier ones, are subject to considerable inaccuracy. Fig. 6 shows the variation in the magnitude of $\Delta\sigma_c$ immediately before each event when a realistic 0.1° inaccuracy is considered. In general, the sensitivity of Coulomb stress change to the location of the epicentre is not too strong, with the exceptions of the 1944 and 1951 events.

5.3. The 1999 İzmit and Düzce events

The most recent earthquakes of the westwards migrating sequence were the 1999 $M_w=7.4$ İzmit/Kocaeli (1999a) and $M_w=7.1$ Düzce (1999b) events. Fig. 7 shows the state of the total cumulative $\Delta\sigma_c$ field for optimally oriented fault planes, as well as the stress load on the rupture surfaces, immediately before both events. We assumed a 10 MPa uniaxial compression N120°E oriented regional stress field for the calculation of the optimally oriented fault planes (Stein et al., 1997; Hubert-Ferrari et al., 2000; Pinar et al., 2001). Most of the surface of the faults involved in the 1999a event were subjected to high Coulomb stresses at the moment of the earthquake (Fig. 7a). With the exception of the Sapanca–Akyazi segment, the rest of the rupture length were loaded with stress values over 0.1 MPa. Moreover, the İzmit–Sapanca Lake segment, were the epicentre was located, as well as its surroundings, were subjected to stresses over 0.3 MPa. The 1999b rupture was also mostly loaded, although the Coulomb stresses in this area were partially released by the 1944, 1957 and 1967 events. The stress changes caused by the 1999a shock induced important changes on the 1999b rupture.

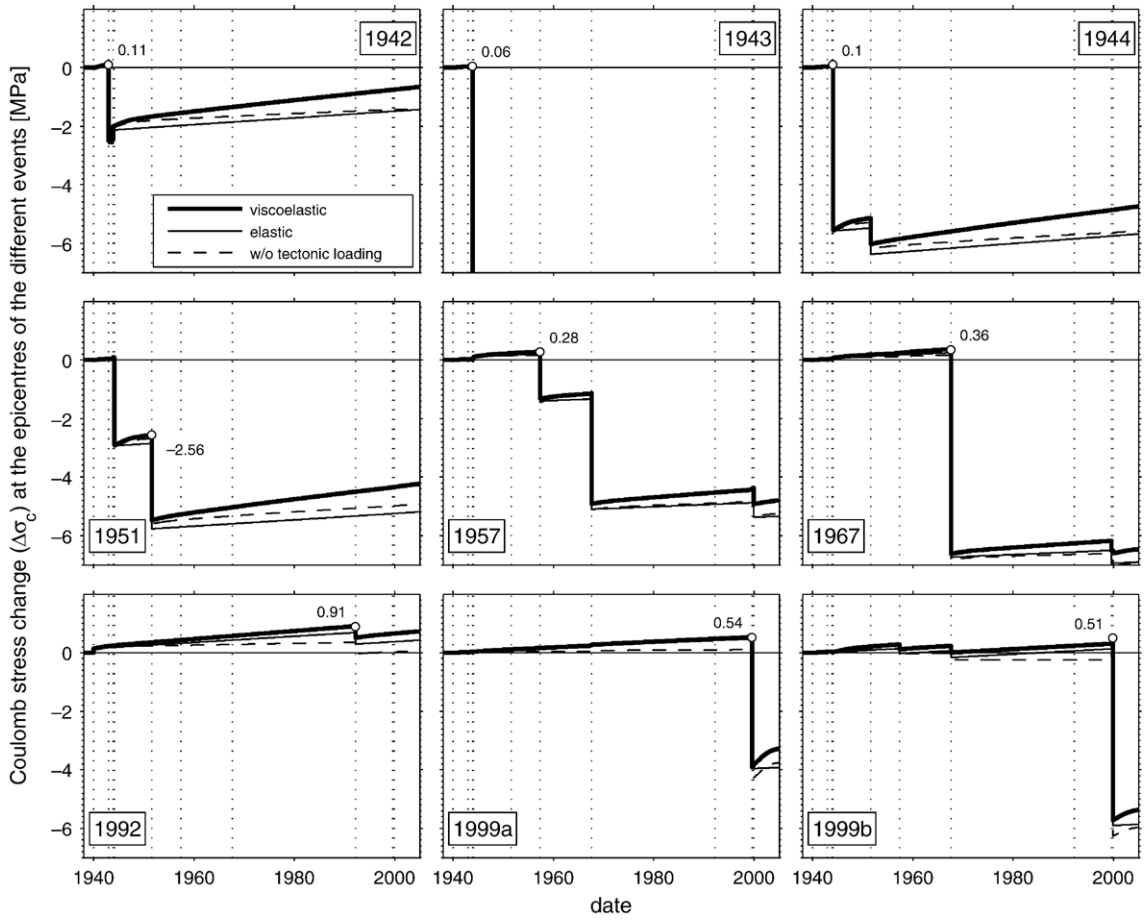

Fig. 5. Time-evolution of Coulomb stress on the epicentres of the considered events (Table 1). Vertical dotted lines mark the timing of each event considered. The thick solid line shows the stress development when elastic and viscoelastic stress changes, as well as tectonic loading, are considered. The thin solid line shows the development when the effect from viscoelastic relaxation is not considered. The thin dashed line displays the case where viscoelastic relaxation is considered but tectonic loading is not. The white dot marks the moment and state of stress at the epicentre when the rupture occurs. The value marked close to the dot is the Coulomb stress at that moment, in MPa.

Stresses on the later rupture were larger than before the 1999a shock took place (Fig. 7b), including at the event's epicentre (Fig. 5).

The local $M \geq 2$ seismicity (KOERI, 2005) correlated with the state of the $\Delta\sigma_c$ field before the 1999a event (Fig. 7a). In addition, there was an important cluster of activity in the place where the epicentre of the 1999a event was going to take place. After this event and before the 1999b event the correlation is less apparent (Fig. 7b). It should be noted that the displayed seismicity ranges from 0 to 17 km depth. For deeper regions, the calculated $\Delta\sigma_c$ field may not be representative.

5.4. The Marmara Sea region

The current situation in the Marmara Sea region according to our computations is displayed in Fig. 8a, for optimally oriented fault planes and for the two segments of the NAF in the region. We assumed a 10 MPa uniaxial compression N120°E oriented regional stress field. The effect of the M_s=6.4 1963 Cinarcik event (Ambraseys and Jackson, 2000) was taken into account, since its influence in the region may not be negligible.

Most of the region shows high stress values. The effect of tectonic loading (Fig. 8b, for 10 years), is not as important as the stress changes induced by post-seismic stress relaxation. Fig. 8c and d, respectively 5 and 10 years after the last event of the sequence, show that the viscoelastic relaxation increases the stresses in the region at a faster rate than steady tectonic loading.

The local $M \geq 2$ seismicity between 0 and 17 km deep (KOERI, 2005) correlates with the calculated Coulomb stress change, with high activity rates

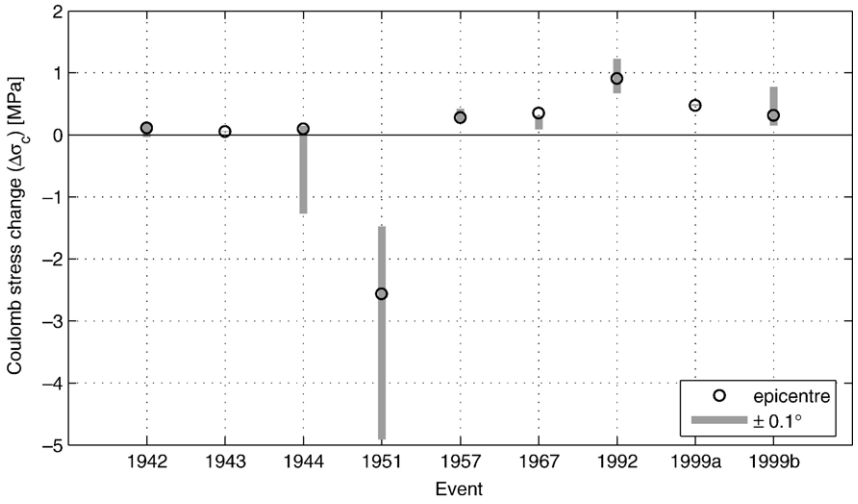

Fig. 6. Variation of the Coulomb stress changes when possible inaccuracies in the epicentral location are considered. The circle shows the $\Delta\sigma_c$ value for the epicentral location provided by the corresponding catalogue (see Table 1). The grey line displays the variation when this location is changed by 0.1° in any direction.

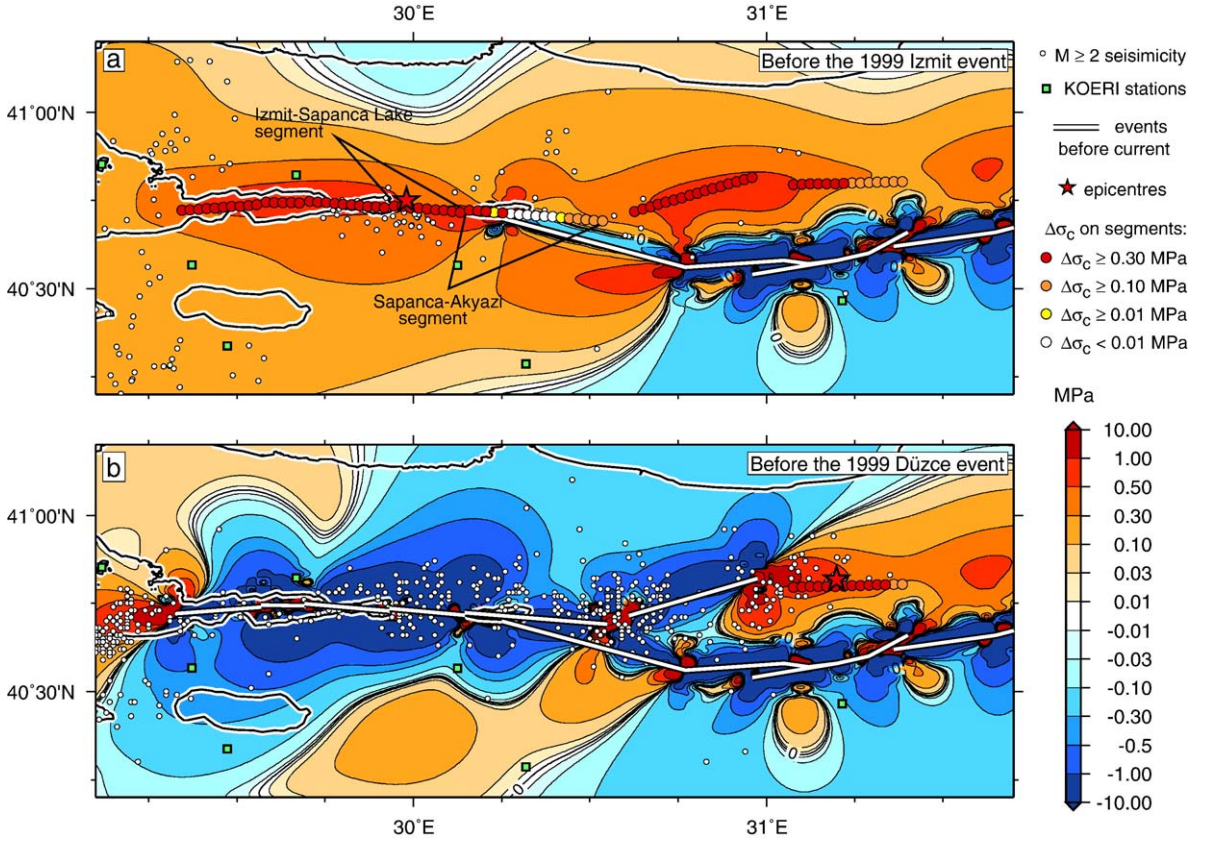

Fig. 7. Coulomb stress change at 10 km depth on optimally oriented fault planes (colour field, 10 MPa uniaxial compression, N120°E oriented regional stress field) and on given faults (filled circles). (a) shows the situation before the August 17th, 1999 event (1999a), and (b) before the November 12th, 1999 shock (1999b). White lines are already ruptured segments. Red stars display the location of the epicentres. Small white dots show the local $M \geq 2$ seismicity at depths between 0 and 17 km over six months before the 1999a event (a) and for the period between the 1999a and 1999b shocks (b). Green squares display the location of the Kandilli Observatory and Earthquake Research Institute (KOERI) seismic stations.

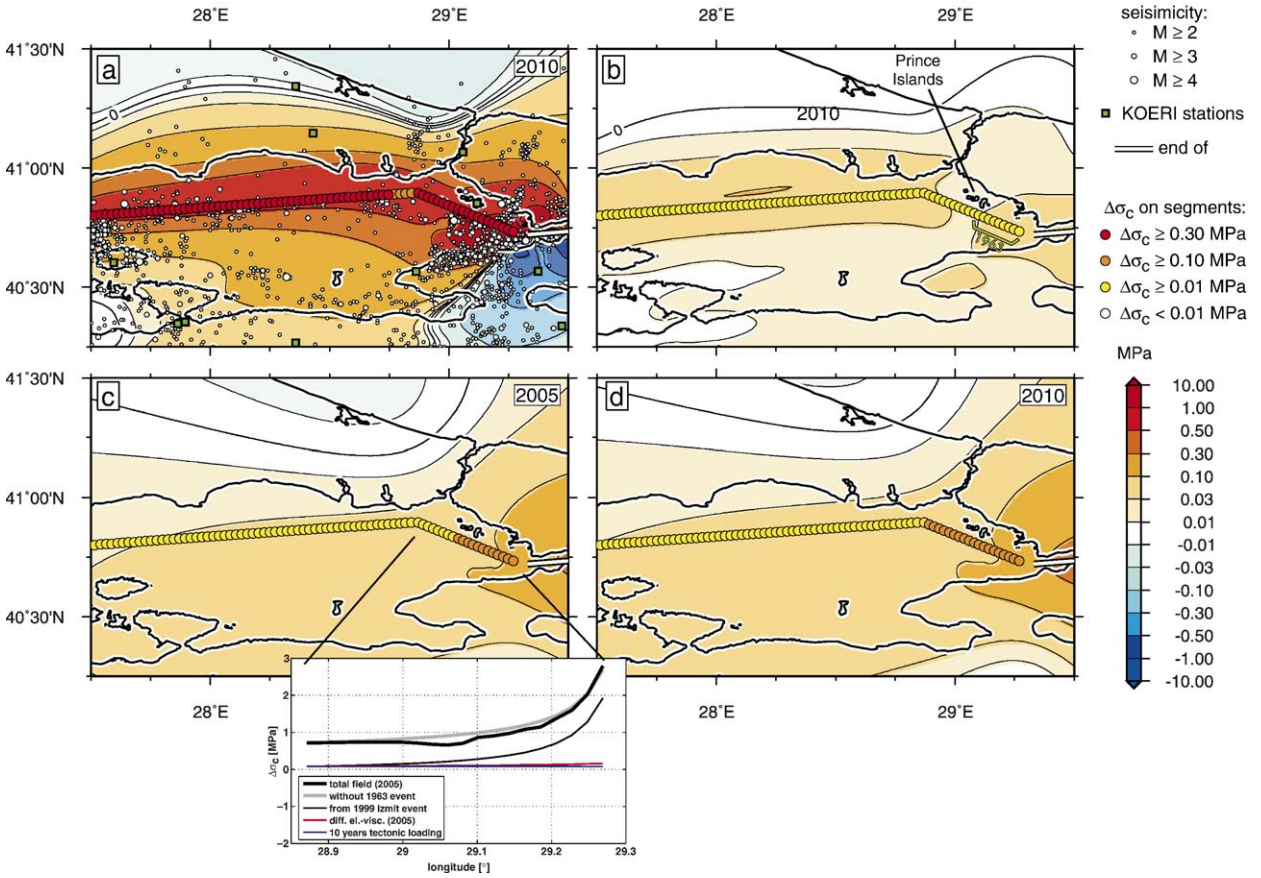

Fig. 8. Coulomb stress change at 10 km depth on optimally oriented fault planes (colour field, 10 MPa uniaxial compression, N120°E oriented regional stress field), and on given faults (filled circles). The 1963 M_s=6.4 Cinarcik earthquake rupture surface is marked in (b), south west of the Prince Islands. The total stress field is displayed in (a); (b) shows the change in Coulomb stresses due to 10 years of steady tectonic loading; (c) and (d) show the cumulative effect of viscoelastic relaxation, for the present time and in 2010, respectively. The white line displays the western end of the 1999a rupture. Small white dots in (a) show the local $M \geq 2$ seismicity for the period 2000–2004 at depths between 0 and 17 km. Green squares display the location of the Kandilli Observatory and Earthquake Research Institute (KOERI) seismic stations. The inset in (c) shows the total $\Delta\sigma_c$ for the Prince Islands segment in 2005 (black thick line), when the 1963 Cinarcik event is not considered (grey thick line), the coseismic contribution from the 1999 İzmit shock (black thin line), the contribution from viscoelastic relaxation (red line) and the changes corresponding to 10 years of tectonic loading (blue line).

associated with the lobe of large $\Delta\sigma_c$ values at the western end of the 1999a rupture ($\Delta\sigma_c \geq 0.3$ MPa), and more activity, in general, for areas with $\Delta\sigma_c \geq 0.1$ MPa.

6. Discussion

6.1. Coulomb stress on the rupture surfaces and at the epicentres

In general, the Coulomb stress criterion explains the triggering of subsequent earthquakes by preceding ones. Almost all rupture surfaces, or a large percentage of them, and/or their epicentres, were strongly stressed at the moment of the shock (Table 3 and Fig. 5). The results for the epicentres are stable with respect to the possible inaccuracies in their location (Fig. 6), with the exception of the 1944 and 1951 earthquakes. The 1944 epicentre was located very close to previous ruptures (1943, which took place only 2 months before the 1944). Close to the rupture, the stress change gradient is very high, hence the position of the epicentre plays a major role. At the epicentre of the 1951 event, $\Delta\sigma_c$ is strongly negative, independent of variation in its location.

It should be noted that only the ruptures of the 1944, 1957, 1992 and 1999b events were stressed over their whole surfaces under certain conditions (Table 3). For most of the events, the rest of the surface was probably dynamically activated during the shock, as described by the general asperity model (Lay and Kanamori, 1981). With the exception of the 1942 earthquake, over 75% of

the events' ruptures was stressed before the event. This coincide with the results of Steacy and McCloskey (1998), according to which large events only occur when the entire fault is highly stressed relative to its strength. In general, the percentage of stressed surface does not change drastically with the viscosity chosen, and values lower than 10^{18} Pa·s for the weak layer do not lead to noteworthy improvements.

The rupture of the 1992 event was strongly stressed over its whole surface, independently of the model assumptions. The stress at the epicentre reached 0.91 MPa before the shock. However, a potentially important factor is the seismicity further to the east, and on the EAF, south of the 1992 shock. At least 3 strong events took place in these areas between 1939 and 1992, in 1949, 1966 and 1971 (Dewey, 1976), and they may have had a significant influence on the Coulomb stress on the 1992 rupture surface. In addition, recent studies show that fault distribution in the region east of the 1992 event might be more complex than the one traditionally assumed (Milkereit et al., 2004). Other authors suggest that deep steady slip may not be adequate to estimate the stress changes due to steady tectonic loading in this region (Nalbant et al., 2005a,b). For these reasons, it is unlikely that we would improve our understanding of this region by broadening our study area further to the east. Other than this, it would introduce several additional unknown parameters into our study. Measurements and estimates of the slip on the surface of the 1939 event are insufficient (Barka, 1996), and the 1992 event did not provide surface expressions of the rupture (Grosser et al., 1998), so that the present results about the 1992 event should be treated carefully. A more detailed study, similar to the one carried out by Nalbant et al. (2005a,b), would be necessary to better understand the influence of viscoelastic relaxation in this area.

We observed that tectonic loading and viscoelastic relaxation increased the stressed surface by a comparable percentage, with the exception of the 1943, 1944 and 1999b events (Table 3). For these three earthquakes, the effect of steady tectonic loading is much more important than that from viscoelastic relaxation. For the 1943 and 1944 events, this is due to two factors: first, the time interval between these shocks and earlier events in the sequence is too short for viscoelastic relaxation to have a more important effect (Fig. 5); second, the rupture surfaces of these earthquakes were notable long, with mainly their easternmost ends loaded by the previous ruptures. For these two events, as well as for the 1939 earthquake, the steady tectonic loading during the preceding centuries seems to be the determining factor for the extension of the rupture surface, rather than the calculated Coulomb stress changes. The case of the 1999b earthquake appears to be different. For this event, the elastic/coseismic stress changes only manage to stress 7% of the rupture surface. The effect of viscoelastic relaxation since 1939 is about 0.3 MPa (see Fig. 4). When combined with the viscoelastic stress changes only 21–29% of the rupture surface overcomes the threshold value of 0.01 MPa (Table 3). The tectonic loading, on the contrary, rises the percentage of stressed surface from 7% to 100%.

The 1951 event presents a rupture surface that is totally unloaded, independent of the assumptions made. This, together with the results for the 1951 epicentre, indicates that the Coulomb stress change approach, as applied in this study, cannot offer a plausible explanation for the occurrence of this event. Some authors model this shock as a reverse slip event (Stein et al., 1997), striking parallel to the NAF. We could not find any evidence in the literature to support this possibility. On the contrary, the fault plane solution for this event is that of a strike–slip event (McKenzie, 1972; Sengör et al., 2005), and the studies of the surface expression of the rupture also deny the existence of significant reverse slip (Pinar, 1953; Barka and Kadinsky-Cade, 1988). In addition to the poorly known geometry and mechanism of the 1951 shock, it is possible that creep occurring on part of the 1944 rupture (Ambraseys, 1970; Kondo et al., 2005) may have played a role in the triggering of the 1951 event.

We tested the stability of our results by comparing different models. The role of the effective coefficient of friction is not trivial, as it modulates the contribution of the normal stress to the Coulomb stress. For most of the earthquakes studied in this work, the influence of the value for μ' is very limited (Table 4a), with the exception of the 1942, 1943 and both 1999 events, for which some model assumptions cause noteworthy changes. The reason for this is the relative location of the rupture surfaces. At the centre of the study region, the events in the sequence fall in line along the NAF, with each event's rupture adjacent to the previous ones. Normal stresses are small in this direction, hence Coulomb stress change is basically governed by shear stress change, and the influence of μ' disappears. Other than this, the westernmost part of the 1939 rupture occurred south from the main NAF (Barka, 1996), as well as south from the future 1943 and 1944 ruptures. Similarly, the 1999 events took place in a region where the geometry of the NAF is more complicated and shocks did not line up along the same main fault. Normal stress field gains importance when calculating

$\Delta\sigma_c$ in this circumstances, and the choice for the value of μ' has a consequence on the results.

Changes in the properties of the medium (Table 4b and c) also led to punctual changes in the results. Results for Model 3 are lower than those for Model 1, although not drastically, while Model 2 gave results that differ significantly from those of Model 1. However, the percentage of the stressed area on the rupture surfaces does not systematically increase or decrease between the models, so that we cannot extract information about the rheological stratification of the region from the analysis of the Coulomb stress changes.

6.2. The 1999 İzmit and Düzce events

If we assume that an important part of the rupture surface must be stressed for an earthquake to take place, then Model 2 with $\eta_{lc}=10^{18}$ Pa·s or Model 1 with $\eta_m=5\cdot10^{17}$–10^{18} Pa·s are the favoured models to explain the triggering of the 1999a event. In these cases, 91–94% of the rupture is stressed (Tables 3 and 4). However, the difference in the results from among the models and viscosity values is not strong. When tectonic loading is considered in addition to the earthquake related coseismic changes, the stressed surface increases from 49% to 85%. A similar increase takes place when relaxation is taken into account, with the result of 81% of the surface being stressed.

When only the coseismic stress change due to previous events is considered, only 7% of the 1999b rupture surface is brought over the threshold value of $\Delta\sigma_c \geq 0.01$ MPa (Table 3). When the effects of viscoelastic relaxation are also considered, the Coulomb stress change increases by an average of 0.2 MPa, and the percentage of the stressed surface raises to 29%. This increase in the Coulomb stress is comparable to 20 years of tectonic loading.

Other time-dependent processes, such as afterslip, ductile creep at depth or poroelastic diffusion processes, may have played an important role in the triggering of the 1999b event (Bürgmann et al., 2002; Hearn et al., 2002). Hearn et al. (2002) analysed the observed post-seismic GPS deformation between the 1999a and 1999b earthquakes to evaluate which process could better explain the occurrence of the 1999b shock. They conclude that the most likely explanation is velocity-strengthening frictional afterslip, and favour this possibility against viscoelastic lower crust relaxation. The viscosity for the lower crust needed to reproduce the fit obtained by means of frictional afterslip models is $\eta=10^{17}$ Pa·s. The authors argue that this value is much lower than most previous estimates of crustal viscosity. However, they do not consider the effects of viscoelastic relaxation in lower layers, although they point out that similar horizontal displacements are obtained when the ratio between viscosity and layer thickness is kept constant and the top of the viscoelastic layer unchanged. Our analysis of the stress field shows that the effect of a viscoelastic half-space (not only a viscoelastic layer) underlying the elastic layers is not negligible. A similar result can be expected for the surface displacement field (Lorenzo-Martín et al., 2006), hence it appears more realistic to include the viscoelastic behaviour of lower regions of the crust and upper mantle when modelling these displacements.

Using an elastic medium and vertical fault planes, Bürgmann et al. (2002) interpreted the post-seismic deformation with afterslip on the 1999a rupture and its prolongation in the E–W direction and with depth. According to their results, rapid slip took place at depth below the eastern part of the 1999a rupture. This would create additional stress on the future 1999b rupture surface, being therefore a potential explanation for the time delay between both 1999 events. Also, poroelastic rebound has proven to have an important role in the first months after an earthquake (Peltzer et al., 1998; Jonsson et al., 2003). Given the short time interval between the 1999a and 1999b events, it might be necessary to consider its influence. However, Hearn et al. (2002) showed that the deformation caused by poroelastic rebound alone cannot explain the measured deformation. From these previous works and the results presented here, it is most likely that the time delay between the 1999 İzmit and the 1999 Düzce events, as well as the time evolution of the observed deformation can only be explained as a combination of several different time-dependent processes.

Utkucu et al. (2003) carried out an analysis of the Coulomb stress state on the 1999 Düzce rupture surface under different conditions. Using an elastic half-space model, they found that the 1999 İzmit event increased the stress on most of the future 1999 Düzce rupture surface, with values for $\Delta\sigma_c$ over 1.2 MPa, with most of the rupture surface stressed between 0 and 0.4 MPa. According to our results, the Coulomb stress increase ranges between 0.25 and 0.05 MPa, from west to east on the 1999 Düzce rupture surface. The difference is due to the different rupture segments used by Utkucu et al. (2003) and in the present study. Utkucu et al. (2003) considered a small eastern segment striking E–W at the end of the 1999 İzmit rupture. However, the observed slip in that area is very small (Barka et al., 2002), and it may be a secondary effect of the 1999 İzmit shock. We used the geometry obtained from the inversion of

InSAR data (Wright et al., 2001), that fitted the observed deformation field without the need of an eastern E–W striking segment.

When the effect of previous events is also considered, we find that the stressed surface decreases notably, in accordance with the results of Utkucu et al. (2003). However, the influence of tectonic loading is very different. This is due to the different elements used to model the tectonic movements. Utkucu et al. (2003) consider a simplified geometry for the long-term tectonic loading model, whereas we used the more detailed results from Flerit et al. (2003, 2004), based on GPS velocity vectors compiled by McClusky et al. (2000). Utkucu et al. (2003) model uses a plate rate of 24 mm/a along the Mudurnu Valley, where the 1967 earthquake took place. According to Flerit et al. (2003, 2004), it is more appropriate to split the 24 mm/a in this area into two branches with 12 mm/a each (Fig. 2c), the northernmost of which runs below the 1999b Düzce fault.

6.3. The Marmara Sea region

The local seismicity in the Marmara Sea region correlates with the Coulomb stress change (Fig 7a). A purely elastic approach when calculating the state of the stress field neglects the important stress changes due to viscoelastic relaxation. These process loaded the eastern part of the Marmara Sea region with stresses over 0.1 MPa (Fig. 8c). Also, the viscoelastic effect is comparable or even larger than the stress increase due to 10 years of tectonic loading (compare Fig. 8b and c). Both processes generate stress changes that differ in their pattern: the influence of viscoelastic relaxation is more important to the east of the Marmara Sea region, whereas tectonic loading increases σ_c in a more homogeneous way. The eastern segment of the NAF in the Marmara Sea, which was already strongly stressed ($\Delta\sigma_c \geq 0.3$ MPa, Fig. 8a), is currently being loaded at a much faster rate than would be expected due to tectonic loading alone (Fig. 8c and d). Accordingly, stress changes due to viscoelastic relaxation should be taken into account in studies focusing on the state of the Coulomb stress field in this region.

Most of the NAF in the Marmara Sea is currently strongly loaded ($\Delta\sigma_c \geq 0.3$ MPa), and the whole region displays $\Delta\sigma_c$ values up to 1 MPa. These results agree with those of Hubert-Ferrari et al. (2000). Their study also shows that aftershocks immediately after the 1999 İzmit event are absent in the area where the 1963 Cinarcik earthquake released stress. We find that the combined effect of the 1999 İzmit earthquake, tectonic loading and viscoelastic relaxation erased in the mean time any possible stress shadow around the area where the 1963 Cinarcik event took place (Fig. 8a). The fact that local seismicity between 2000 and 2004 does not show any noticeable decrease in this area reflects this change in the Coulomb stress field between 1999 and the present date.

When the effects of the 1963 event are not considered, Coulomb stress changes on the Prince Islands segment range from 0.73 to 2.68 MPa (Fig. 8, inset). Coseismic stress changes due to the 1999 İzmit earthquake range from 0.08 to 1.93 MPa, which is higher in the eastern end than the values estimated by Hubert-Ferrari et al. (2000, 0–0.5 MPa) or Parsons (2004, 0.02–0.760 MPa). Hubert-Ferrari et al. (2000) considered a 1999 İzmit rupture surface shorter to the west than that suggested by later studies (Reilinger et al., 2000; Wright et al., 2001). Parsons (2004) considered different slip distributions for the 1999 İzmit rupture surface, other than the one used in the present study (Wright et al., 2001). More detailed slip distributions (Reilinger et al., 2000; Delouis et al., 2002) suggest less slip to the western end of the 1999 İzmit rupture, so that Coulomb stress change in the immediacy of the fault's end would also be proportionally smaller. However, there is still no agreement on the slip distribution of the 1999 İzmit earthquake (Reilinger et al., 2000; Bouchon et al., 2002; Delouis et al., 2002). In addition, the effect from details of the slip distribution vanish with distance from the rupture. Pollitz and Sacks (2002) found that the static stress pattern around the 1992 Landers rupture was sensitive to the choice of the slip model, but the post-seismic stress change depended little on this choice. The use of a simple slip model for the present study is therefore justified.

Ten years of tectonic loading causes a stress increase of 0.08 MPa along the Prince Islands segment (Fig. 8, inset, blue line). Sixty six years of tectonic loading plus the coseismic effect of the 1999 İzmit earthquake create 0.52–2.37 MPa, which is comparable to the 0.5–1 MPa obtained by Utkucu et al. (2003) using the slip distribution model of Delouis et al. (2002). The contribution due to the post-seismic viscoelastic relaxation between 1999 and 2005 (Fig. 8, inset, red line) ranges from 0.12 to 0.27 MPa, equivalent to 15 to 35 years of tectonic loading.

7. Conclusions

Our analysis presents several improvements in relation to previous works. We consider a whole sequence of earthquakes instead of single pairs of

events, we used a horizontally stratified medium and include the time-dependent effects of viscoelastic relaxation. Our results show that the effects of the latter are comparable or even greater in magnitude than the stress changes induced by steady tectonic loading during the interseismic phase of the earthquake cycle (Figs. 4, 5 and 8). Viscoelastic relaxation should therefore not be neglected.

The Coulomb stress failure criterion provides good results in this area and for this sequence of events, but considering only elastic stress changes can neglect an important part of the actual stress increase/decrease. For the case of the Marmara Sea region, the current rate of stress loading is governed by viscoelastic relaxation rather than tectonic loading. Accordingly, this result should be taken into account by seismic-hazard assessment studies in this region.

There is the possibility that our modelling approach is still too coarse for these events or this region, and that a more exhaustive analyses should be carried out, taking into account a more detailed geometry and slip distribution for the events and/or additional information about the rheological properties of the lower crust and upper mantle in the area. Nevertheless, it is improbable that the importance of the viscoelastic relaxation shown here would decrease considerably when including more detailed model parameters. The viscoelastic relaxation process should therefore be considered when analysing time-dependent deformation-related data.

Acknowledgments

We wish to thank Suleyman S. Nalbant and an anonymous reviewer for thoughtful comments on the manuscript, that lead to significant improvement in the quality of the present work. We are also grateful to Roland Bürgmann, Helmut Grosser, Stefano Parolai and Sandra Richwalski for discussions and advice about the manuscript. This work was supported by the Deutsche Forschungsgemeinschaft under grant SFB 526 (Collaborative Research Centre 'Rheology of the Earth — from the Upper Crust to the Subduction Zone', subproject C5) at the Ruhr University Bochum, and by the GeoForschungsZentrum Potsdam.

References

Alsan, E., Tezucan, L., Bath, M., 1976. An earthquake catalogue for Turkey for the interval 1913–1970. Tectonophysics 31 (1–2), T13–T19.

Ambraseys, N.N., 1970. Some characteristic features of the Anatolian fault zone. Tectonophys 9, 143–165.

Ambraseys, N., 2002. The seismic activity of the Marmara Sea region over the last 2000 years. Bull. Seismol. Soc. Am. 92 (1), 1–18.

Ambraseys, N.N., Finkel, C.F., 1991. Long-term seismicity of Istanbul and of the Marmara Sea region. Terra Nova 3 (5), 527–539.

Ambraseys, N.N., Finkel, C.F., 1995. The Seismicity of Turkey and Adjacent Areas — A Historical Review, 1500–1800. M. S. Eren Publications and Books, Istanbul.

Ambraseys, N.N., Jackson, J.A., 2000. Seismicity of the Sea of Marmara (Turkey) since 1500. Geophys. J. Int. 141 (3), F1–F6.

Ambraseys, N.N., Zatopek, A., 1969. The Mudurnu valley, west Anatolia, Turkey, earthquake of 22 July 1967. Bull. Seismol. Soc. Am. 59 (2), 521–589.

Armijo, R., Flerit, F., King, G., Meyer, B., 2003. Linear elastic fracture mechanics explains the past and present evolution of the Aegean. Earth Planet. Sci. Lett. 217 (1–2), 85–95.

Armijo, R., Pondard, N., Meyer, B., Uçarkus, G., Lépinay, B.M.d., Malavieille, J., Dominguez, S., Gustcher, M.-A., Schmidt, S., Beck, C., Çagatav, N., Çakir, Z., Imren, C., Eris, K., Natalin, B., Özalaybey, S., Tolun, L., Lefèvre, I., Seeber, L., Gasperini, L., Rangin, C., Emre, O., Sarikavak, K., 2005. Submarine fault scarps in the Sea of Marmara pull-apart (North Anatolian Fault): implications for seismic hazard in Istanbul. Geochem. Geophys. Geosyst. 6 (6), Q06009, doi:10.1029/2004GC000896.

Ayhan, M.E., Buergmann, R., McClusky, S., Lenk, O., Aktug, B., Herece, E., Reilinger, R.E., 2001. Kinematic of the M_w=7.2, 12 November 1999, Duzce, Turkey earthquake. Geophys. Res. Lett. 28 (2), 367–370.

Barka, A., 1996. Slip distribution along the North Anatolian fault associated with large earthquakes of the period 1939–1967. Bull. Seismol. Soc. Am. 86, 1238–1254.

Barka, A., Kadinsky-Cade, K., 1988. Strike–slip fault geometry in Turkey and its influence on earthquake activity. Tectonics 7, 663–684.

Barka, A.A., Akyuz, H.S., Altunel, E., Sunal, G., Cakir, Z., Dikbas, A., Yerli, B., Armijo, R., Meyer, B., de, C.J.B., Rockwell, T.K., Dolan, J.R., Hartleb, R.D., Dawson, T.E., Christofferson, S.A., Tucker, A., Fumal, T.E., Langridge, R.M., Stenner, H.D., Lettis, W., Bachhuber, J., Page, W.D., 2002. The surface rupture and slip distribution of the 17 August 1999 Izmit earthquake (M 7.4). North Anatolian Fault. Bull. Seismol. Soc. Am. 92 (1), 43–60.

Barrientos, S.E., Plafker, G., Lorca, E., 1992. Postseismic coastal uplift in Southern Chile. Geophys. Res. Lett. 19, 701–704.

Beeler, N.M., Simpson, R.W., Hickman, S.H., Lockner, D.A., 2000. Pore fluid pressure, apparent friction, and Coulomb failure. J. Geophys. Res., B Solid Earth 105 (11).

Belardinelli, M.E., Cocco, M., Coutant, O., Cotton, F., 1999. Redistribution of dynamic stress during coseismic ruptures: evidence for fault interaction and earthquake triggering. J. Geophys. Res. 104 (B7), 14925–14945.

Belardinelli, M.E., Bizzarri, A., Cocco, M., 2003. Earthquake triggering by static and dynamic stress changes. J. Geophys. Res., 108 (B3): ESE 1-1 to ESE 1-16.

Bouchon, M., Toksöz, M.N., Karabulut, H., Bouin, M.-P., Dietrich, M., Aktar, M., Edie, M., 2002. Space and time evolution of rupture and faulting during the 1999 the Izmit (Turkey) earthquake. Bull. Seismol. Soc. Am. 92 (1), 256–266.

Bürgmann, R., Ergintav, S., Segall, P., Hearn, E.H., McClusky, S., Reilinger, R.E., Woith, H., Zschau, J., 2002. Time-dependent distributed afterslip on and deep below the Izmit earthquake rupture. Bull. Seismol. Soc. Am. 92 (1), 126–137.

Byerlee, J., 1978. Friction of rocks. PAGEOPH 116, 615–626.
Cakir, Z., Barka, A.A., Evren, E., 2003. Coulomb stress interactions and the 1999 Marmara earthquakes. Turk. J. Earth Sci. 12 (1), 91–103.
Casarotti, E., Piersanti, A., 2003. Postseismic stress diffusion in Chile and South Peru. Earth Planet. Sci. Lett. 206 (3–4), 325–333.
Christensen, R.M., 1982. Theory of Viscoelasticity. An Introduction, second ed. Academic Press, New York.
Cocco, M., Rice, J.R., 2002. Pore pressure and poroelasticity effects in Coulomb stress analysis of earthquake interactions. J. Geophys. Res., B Solid Earth 107 (2), 2–1.
Cohen, S.C., 1982. A multilayer model of time-dependent deformation following an earthquake on a strike–slip fault. J. Geophys. Res. 87 (B7), 5409–5421.
Delouis, B., Giardini, D., Lundgren, P., Salichon, J., 2002. Joint inversion of InSAR, GPS, teleseismic, and strong-motion data for the spatial and temporal distribution of earthquake slip: application to the 1999 Izmit mainshock. Bull. Seismol. Soc. Am. 92 (1), 278–299.
Deng, J., Gurnis, M., Kanamori, H., Hauksson, E., 1998. Viscoelastic flow in the lower crust after the 1992 Landers, California, earthquake. Science 282 (5394), 1689–1692.
Deng, J., Hudnut, K., Gurnis, M., Hauksson, E., 1999. Stress loading from viscous flow in the lower crust and triggering of aftershocks following the 1994 Northridge, California, earthquake. Geophys. Res. Lett. 26 (21), 3209–3212.
Dewey, J.W., 1976. Seismicity of northern Anatolia. Bull. Seismol. Soc. Am. 66, 843–868.
Fernández, J., Rundle, J.B., 2004. Postseismic viscoelastic-gravitational half space computations: problems and solutions. Geophys. Res. Lett. 31 (7).
Fernández, J., Yu, T.-T., Rundle, J.B., 1996. Deformation produced by a rectangular dipping fault in a viscoelastic-gravitational layered Earth model: Part I. Thrust fault FLTGRV and FLTGRH FORTRAN programs. Comput. Geosci. 22, 735–750.
Flerit, F., Armijo, R., King, G.C.P., Meyer, B., Barka, A., 2003. Slip partitioning in the Sea of Marmara pull-apart determined from GPS velocity vectors. Geophys. J. Int. 154 (1), 1–7.
Flerit, F., Armijo, R., King, G., Meyer, B., 2004. The mechanical interaction between the propagating North Anatolian Fault and the back-arc extension in the Aegean. Earth Planet. Sci. Lett. 224 (3–4), 347–362.
Freed, A.M., 2005. Earthquake triggering by static, dynamic and postseismic stress transfer. Annu. Rev. Earth Planet. Sci. 33, 335–367.
Freed, A.M., Bürgmann, R., 2004. Evidence of power-law flow in the Mojave desert mantle. Nature 430 (6999), 548–551.
Freed, A.M., Lin, J., 2001. Delayed triggering of the 1999 Hector Mine earthquake by viscoelastic stress transfer. Nature 411 (6834), 180–183 (See also: E. Harding Hearn, Nature, same issue, p. 150.).
Gokasan, E., Ustaömer, T., Gazioglu, C., Yucel, Z.Y., Öztürk, K., Tur, H., Ecevitoglu, B., Tok, B., 2003. Morpho-tectonic evolution of the Marmara Sea inferred from multi-beam bathymetric and seismic data. Geo Mar. Lett. 23 (1), 19–33.
Grosser, H., Baumbach, M., Berckhemer, H., Baier, B., Karahan, A., Schelle, H., Krueger, F., Paulat, A., Michel, G., Demirtas, R., Gencoglu, S., Yilmaz, R., 1998. The Erzincan (Turkey) earthquake (M (sub s) 6.8) of March 13, 1992 and its aftershocks sequence. Pure Appl. Geophys. 152 (3), 465–505.
Hardebeck, J.L., 2004. Stress triggering and earthquake probability estimates. J. Geophys. Res. 109 (B4).
Harris, R.A., 1998. Introduction to special section: stress triggers, stress shadows, and implications for seismic hazard. J. Geophys. Res. 103 (B10), 24347–24358.
Harris, R.A., Simpson, R.W., Reasenberg, P.A., 1995. Influence of static stress changes on earthquake locations in southern California. Nature 375 (6528), 221–224.
Healy, J.H., Rubey, W.W., Griggs, D.T., Raleigh, C.B., 1968. The Denver earthquakes. Science 161, 1301–1310.
Hearn, E.H., Bürgmann, R., Reilinger, R.E., 2002. Dynamics of Izmit earthquake postseismic deformation and loading of the Düzce earthquake hypocenter. Bull. Seismol. Soc. Am. 92 (1), 172–193.
Horasan, G., Gulen, L., Pinar, A., Kalafat, D., Ozel, N., Kuleli, H.S., Isikara, A.M., 2002. Lithospheric structure of the Marmara and Aegean regions, western Turkey. The Izmit, Turkey, earthquake of 17 August 1999. Seismological Society of America, Berkeley, CA, United States, pp. 322–329.
Hubert-Ferrari, A., Barka, A., Jacques, E., Nalbant, S.S., Meyer, B., Armijo, R., Tapponnier, P., King, G.C.P., 2000. Seismic hazard in the Marmara Sea region following the 17 August 1999 Izmit earthquake. Nature 404 (6775), 269–273.
Jackson, J., McKenzie, D., 1988. The relationship between plate motions and seismic moment tensors, and the rates of active deformation in the Mediterranean and Middle East. Geophys. J. 93, 45–73.
Jonsson, S., Segall, P., Pedersen, R., Bjornsson, G., 2003. Post-earthquake ground movements correlated to pore-pressure transients. Nature (London) 424 (6945), 179–183.
Karahan, A.E., Berckhemer, H., Baier, B., 2001. Crustal structure at the western end of the North Anatolian fault zone from deep seismic sounding. Annali di Geofisica (1993), 44 (1): 49–68.
Kasahara, K., 1975. Aseismic faulting following the 1973 Nemuro-oki earthquake, Hokkaido, Japan (A possibility). PAGEOPH 113, 127–139.
Kaypak, B., Eyidogan, H., 2005. One-dimensional crustal structure of the Erzincan basin, Eastern Turkey and relocation of the 1992 Erzincan earthquake (M_s=6.8) aftershock sequence. Phys. Earth Planet. Inter. 151, 1–20.
King, G.C.P., Cocco, M., 2001. Fault interaction by elastic stress change: new clues from earthquake sequence. Adv. Geophys. 44, 1–38.
King, G.C.P., Stein, R.S., Lin, J., 1994. Static stress changes and the triggering of earthquakes. Bull. Seismol. Soc. Am. 84, 935–953.
KOERI, 2005. Recent earthquakes in Turkey. Bogazici University, Kandilli Observatory and Earthquake Research Institute. http://www.koeri.boun.edu.tr/sismo/defaulteng.htm.
Kondo, H., Awata, Y., Yoshioka, T., Emre, O., Dog?an, A., O?zalp, S., Tokay, F., Yildirim, C., Okumura, K., 2005. Slip distribution, fault geometry, and fault segmentation of the 1944 Bolu–Gerede earthquake rupture, North Anatolian fault, Turkey. Bull. Seismol. Soc. Am. 95 (4), 1234–1249.
Lay, T., Kanamori, H., 1981. An asperity model of large earthquake sequences. In: Simpson, D.W., Richards, P.J. (Eds.), Earthquake Prediction. Maurice Ewing Series. AGU, Washington, D.C, pp. 579–592.
Le Pichon, X., Sengor, A.M.C., Demirbag, E., Rangin, C., Imren, C., Armijo, R., Gorur, N., Cagatay, N., Mercier, d.L.B., Meyer, B., Saatcilar, R., Tok, B., 2001. The active main Marmara Fault. Earth Planet. Sci. Lett. 192 (4), 595–616.
Lin, J., Stein, R.S., 2004. Stress triggering in thrust and subduction earthquakes and stress interaction between the southern San Andreas and nearby thrust and strike–slip faults. J. Geophys. Res. 109 (B2).

Linde, A.T., Silver, P.G., 1989. Elevation changes and the Great 1960 Chilean earthquake: support for aseismic slip. Geophys. Res. Lett. 16, 1305–1308.

Lorenzo-Martín, F., Roth, F., Wang, R., 2006. Inversion for rheological parameters from postseismic surface deformation associated to the 1960 Valdivia earthquake. Chile. Geophys. J. Int. 164, 75–87.

Ma, K.-F., Chan, C.-H., Stein, R.S., 2005. Response of seismicity to Coulomb stress triggers and shadows of the 1999 M_w=7.6 Chi-Chi, Taiwan, earthquake. J. Geophys. Res., B Solid Earth 110 (5), B05S19, doi:10.1029/2004JB003389.

McCloskey, J., Nalbant, S.S., Steacy, S., 2005. Earthquake risk from co-seismic stress. Nature 434 (7031), 291.

McClusky, S., Balassanian, S., Barka, A., Demir, A., Ergintav, S., Georgiev, I., Gurkan, O., Hamburger, M., Hurst, K., Kahle, H., Kastens, K., Kekelidze, G., King, R., Kotzev, V., Lenk, O., Mahmoud, S., Mishin, A., Nadariya, M., Ouzounis, A., Paradissis, D., Peter, Y., Prilepin, M., Reilinger, R., Sanli, I., Seeger, H., Tealeb, A., Toksöz, M.N., Veis, G., 2000. Global Positioning System constraints on plate kinematics and dynamics in the eastern Mediterranean and Caucasus. J. Geophys. Res. 105 (B3), 5695–5719.

McKenzie, D.P., 1972. Active tectonics of the Mediterranean region. Geophys. J. R. Astron. Soc. 30, 109–185.

Milkereit, C., Zünbül, S., Karakisa, S., Iravul, Y., Zschau, J., Baumbach, M., Grosser, H., Günther, E., Umutlu, N., Kuru, T., Erkul, E., Klinge, K., Ibs-von Seht, M., Karahan, A., 2000. Preliminary aftershock analysis of the M_w=7.4 Izmit and M_w=7.1 Düzce earthquake in western Turkey. In: Barka, A., Kozaci, Ö., Akyüz, S., Altunel, A. (Eds.), The 1999 Izmit and Düzce Earthquakes: Preliminary Results. Istanbul Technical University, pp. 179–187.

Milkereit, C., Grosser, H., Wang, R., Wetzel, H.-U., Woith, H., Karakisa, S., Zünbül, S., Zschau, J., 2004. Implications of the 2003 Bingöl Earthquake for the Interaction between the North and East Anatolian Faults. Bull. Seismol. Soc. Am. 6, 2400–2406.

Mogi, K., 1968. Migration of seismic activity. Bull. Earthq. Res. Inst. 46, 53–74.

Muller, J.R., Aydin, A., Maerten, F., 2003. Investigating the transition between the 1967 Mudurnu Valley and the 1999 Izmit earthquakes along the North Anatolian fault with static stress changes. Geophys. J. Int. 154 (2), 471–482.

Nalbant, S.S., Barka, A.A., Alptekin, Ö., 1996. Failure stress change caused by the 1992 Erzincan earthquake (Ms=6.8). Geophys. Res. Lett. 23, 1561–1564.

Nalbant, S.S., Hubert, A., King, G.C.P., 1998. Stress coupling between earthquakes in northwest Turkey and the north Aegean Sea. J. Geophys. Res. 103 (B10), 24469–24486.

Nalbant, S.S., McCloskey, J., Steacy, S., Barka, A.A., 2002. Stress accumulation and increased seismic risk in eastern Turkey. Earth Planet. Sci. Lett. 195 (3–4), 291–298.

Nalbant, S.S., McCloskey, J., Steacy, S., 2005a. Lessons on the calculation of the static stress loading from the 2003 Bingol, Turkey earthquake. Earth Planet. Sci. Lett. 235, 632–640.

Nalbant, S.S., Steacy, S., McCloskey, J., Sieh, K., Natawidjaja, D., 2005b. Earthquake risk on the Sunda trench. Nature 435 (7043), 756–757.

Nostro, C., Chiaraluce, L., Cocco, M., Baumont, D., Scotti, O., 2005. Coulomb stress changes caused by repeated normal faulting earthquakes during the 1997 Umbria–Marche (central Italy) seismic sequence. J. Geophys. Res., B Solid Earth 110 (5), B05S20, doi:10.1029/2004JB003386.

Parsons, T., 2004. Recalculated probability of M >=7 earthquakes beneath the Sea of Marmara, Turkey. J. Geophys. Res., B Solid Earth 109 (5).

Parsons, T., Toda, S., Stein, R.S., Barka, A., Dieterich, J.H., 2000. Heightened odds of large earthquakes near Istanbul: an interaction-based probability calculation. Science 288 (5466), 661–665.

Peltzer, G., Rosen, P., Rogez, F., Hudnut, K., 1998. Poroelastic rebound along the Landers 1992 earthquake surface rupture. J. Geophys. Res. 103 (B12), 30131–30146.

Pinar, N., 1953. Etude géologique et macrosismique du tremblement du terre de Kusurlu (Anatolie septentrionale) du 13 août 1951. Rev. Fac. Sc. Univ. Istanbul XVIII, 131–142.

Pinar, A., Honkura, Y., Kikuchi, M., 1994. Rupture process of the 1992 Erzincan earthquake and its implication for seismotectonics in eastern Turkey. Geophys. Res. Lett. 21 (18), 1971–1974.

Pinar, A., Honkura, Y., Kuge, K., 2001. Seismic activity triggered by the 1999 Izmit earthquake and its implications for the assessment of future risk. Geophys. J. Int. 146 (1), F1–F7.

Pollitz, F.F., 1992. Postseismic relaxation theory on the spherical earth. Bull. Seismol. Soc. Am. 82, 422–453.

Pollitz, F.F., 1997. Gravitational viscoelastic postseismic relaxation on a layered spherical Earth. J. Geophys. Res. 102 (B8), 17,921–17,941.

Pollitz, F.F., Sacks, I.S., 2002. Stress triggering of the 1999 Hector Mine earthquake by transient deformation following the 1992 Landers earthquake. Bull. Seismol. Soc. Am. 92 (4), 1487–1496.

Pollitz, F.F., Bürgmann, R., Segall, P., 1998. Joint estimation of afterslip rate and postseismic relaxation following the 1989 Loma Prieta earthquake. J. Geophys. Res., B Solid Earth 103 (B11), 26975–26992.

Pollitz, F.F., Wicks, C., Thatcher, W., 2001. Mantle flow beneath a continental strike–slip fault: postseismic deformation after the 1999 Hector Mine earthquake. Science 293 (5536), 1814–1818.

Purcaru, G., Berckhemer, H., 1982. Regularity patterns and zones of seismic potential for future large earthquakes in the Mediterranean region. Tectonophysics 85, 1–30.

Raleigh, C.B., Healy, J.H., Bredehoeft, J.D., 1972. Faulting and crustal stress at Rangely, Colorado. In: Heard, H.C., Borg, I.Y., Carter, N.L., Raleigh, C.B. (Eds.), Flow and Fracture of Rocks. Geophysical Monograph Series. Am. Geophys. Un., Washington, D. C., pp. 275–284.

Reasenberg, P.A., Simpson, R.W., 1992. Response of regional seismicity to the static stress change produced by the Loma Prieta earthquake. Science 255 (5052), 1687–1690.

Reilinger, R.E., Ergintav, S., Buergmann, R., McClusky, S., Lenk, O., Barka, A., Gurkan, O., Hearn, L., Feigl, K.L., Cakmak, R., Aktug, B., Ozener, H., Toksoz, M.N., 2000. Coseismic and postseismic fault slip for the 17 August 1999, M =7.5, Izmit, Turkey earthquake. Science 289 (5484), 1519–1524.

Roth, F., 1988. Modeling of stress patterns along the western part of the North Anatolian Fault Zone. Tectonophysics 152, 215–226.

Saroglu, F., Emre, Ö., Kuscu, I., 1992. Active fault map of Turkey. Geological Research Department of the General Directorate of Mineral Research and Exploration, Ankara, Turkey.

Savage, J.C., 1983. A dislocation model of strain accumulation and release at a subduction zone. J. Geophys. Res. 88, 4984–4996.

Sengör, A.M.C., Görür, N., Saroglu, F., 1985. Strike–slip faulting and related basin formation in zones of tectonic scape: Turkey as a case study. In: Biddle, T.R., Christi-Blick, N. (Eds.), Strike–slip Deformation, Basin Formation and sedimentation. Soc. Econ. Paleontol. Mineral., pp. 227–264.

Sengör, A.M.C., Tüysüz, O., Imren, C., Sakinç, M., Eyidogan, H., Görür, N., Le Pichon, X., Rangin, C., 2005. The North Anatolian Fault: a new look. Annu. Rev. Earth Planet. Sci. 33, 37–112.

Steacy, S.J., McCloskey, J., 1998. What controls an earthquake's size? Results from a heterogeneous cellular automaton. Geophys. J. Int. 133 (1), F11.

Steacy, S., Gomberg, J., Cocco, M., 2005. Introduction to special section: stress transfer, earthquake triggering, and time-dependent seismic hazard. J. Geophys. Res., B Solid Earth 110 (5), B05S01, doi:10.1029/2005JB003692.

Stein, R.S., 1999. The role of stress transfer in earthquake occurrence. Nature 402 (6762), 605–609.

Stein, R.S., King, G.C., Lin, J., 1992. Change in failure stress on the southern San Andreas fault system caused by the 1992 magnitude=7.4 Landers earthquake. Science 258 (5086), 1328–1332.

Stein, R.S., King, G.C.P., Lin, J., 1994. Stress triggering of the 1994 *M* =6,7 Northridge, California, earthquake by its predecessors. Science 265, 1432–1435.

Stein, R.S., Barka, A.A., Dieterich, J.H., 1997. Progressive failure on the North Anatolian fault since 1939 by earthquake stress triggering. Geophys. J. Int. 128 (3), 594–604.

Thatcher, W., Rundle, J.R., 1984. A viscoelastic coupling model for the cyclic deformation due to periodically repeated earthquakes at subduction zones. J. Geophys. Res. 89, 7631–7640.

Tibi, R., Bock, G., Xia, Y., Baumbach, M., Grosser, H., Milkereit, C., Karakisa, S., Zunbul, S., Kind, R., Zschau, J., 2001. Rupture processes of the 1999 August 17 Izmit and November 12 Duzce (Turkey) earthquakes. Geophys. J. Int. 144 (2), F1–F7.

Toda, S., Stein, R.S., Reasenberg, P.A., Dieterich, J.H., Yoshida, A., 1998. Stress transferred by the 1995 *M*(w)=6.9 Kobe, Japan, shock: effect on aftershocks and future earthquake probabilities. J. Geophys. Res., B Solid Earth 103 (B10), 24543–24565.

Toksöz, M.N., Shakal, A.F., Michael, A.J., 1979. Space–time migration of earthquakes along the North Anatolian fault zone and seismic gaps. PAGEOPH 117, 1258–1270.

Umutlu, N., Koketsu, K., Milkereit, C., 2004. The rupture process during the 1999 Düzce, Turkey, earthquake from joint inversion of teleseismic and strong-motion data. Tectonophysics 391, 315–324.

Utkucu, M., Nalbant, S.S., McCloskey, J., Steacy, S., Alptekin, Ö., 2003. Slip distribution and stress changes associated with the 1999 November 12, Düzce (Turkey) earthquake (*Mw*=7.1). Geophys. J. Int. 153 (1), 229–241.

Wang, R., 2005. The dislocation theory: a consistent way for including the gravity effect in (visco)elastic plane-earth models. Geophys. J. Int. 161 (1), 191–196.

Wang, R., Lorenzo Martín, F., Roth, F., 2003. Computation of deformation induced by earthquakes in a multi-layered elastic crust — FORTRAN programs EDGRN / EDCMP. Comput. Geosci. 29 (2), 195–207.

Wang, R., Lorenzo-Martín, F., Roth, F., 2006. A semi-analytical software PSGRN/PSCMP for calculating co- and post-seismic deformation on a layered viscoelastic-gravitational half-space. Comput. Geosci. 32, 527–541.

Wright, T., Fielding, E., Parsons, B., 2001. Triggered slip; observations of the 17 August 1999 Izmit (Turkey) earthquake using radar interferometry. Geophys. Res. Lett. 28 (6), 1079–1082.

Zeng, Y., 2001. Viscoelastic stress-triggering of the 1999 Hector Mine earthquake by the 1992 Landers earthquake. Geophys. Res. Lett. 28 (15), 3007–3010.